European Journal of Pharmaceutics and Biopharmaceutics 225 (2026) 115100

Contents lists available at ScienceDirect

European Journal of Pharmaceutics and Biopharmaceutics

journal homepage: www.elsevier.com/locate/ejpb

Structure–Permeability relationships of Vitamin-B-Based quaternary ammonium salts for oral drug development

Adriana Olejniczak [a], Mara G. Freire [b], Michał Niemczak [a,1,*]

[a] Faculty of Chemical Technology, Poznan University of Technology, Berdychowo 4, Poznan 61-131, Poland
[b] CICECO-Aveiro Institute of Materials, Chemistry Department, University of Aveiro 3810-193 Aveiro, Portugal

ARTICLE INFO

Keywords:
Quaternary ammonium salts
Permeability
PAMPA
Oral delivery
Pharmacokinetics
Surface activity

ABSTRACT

Effective oral drug delivery requires compounds with suitable solubility, permeability, and physicochemical properties to ensure efficient absorption in the gastrointestinal tract. This study evaluates vitamin-derived quaternary ammonium salts (QASs) based on nicotinamide, nicotinic acid, and *p*-aminobenzoic acid, together with their nonionic counterparts, as potential orally administrable molecules. *In silico* pharmacokinetic predictions identified nicotinate QASs as the most promising candidates, exhibiting favorable permeability, intestinal absorption, and solubility profiles. PAMPA experiments confirmed high passive permeability for all compounds, with 6-hour P_{app} values exceeding $1.1 \cdot 10^{-6}$ cm·s^{-1}, and demonstrated that membrane transport depends strongly on alkyl chain length and counterion identity. Permeability decreased notably for derivatives with octyl chains, whereas nicotinate QASs displayed values comparable to diclofenac sodium, and the shortest-chain *p*-aminobenzoate and its nonionic analogue slightly surpassed the reference drug. Surface activity analysis revealed that reductions in solution surface tension significantly enhance membrane transport, overriding limitations associated with increased molecular size. Overall, the synergistic influence of alkyl chain length, anion selection, and surface activity underscores the potential of vitamin-derived QASs as tunable, multifunctional candidates for oral drug development.

1. Introduction

Oral drug administration remains the most convenient and widely used route for therapeutics; yet, achieving adequate intestinal absorption while maintaining favorable pharmacokinetic and safety profiles continues to be a significant challenge [1]. The physicochemical properties of a given compound, including solubility, lipophilicity and ionization, critically influence its ability to permeate biological membranes. Quaternary ammonium salts (QASs) represent a versatile class of molecules with adjustable physicochemical properties. Their amphiphilic character is primarily determined by the structure of the quaternary ammonium cation, particularly the balance between the polar headgroup and the hydrophobic alkyl chain length, while the choice of counterion can influence solubility and related characteristics [2–5]. These structural modifications directly influence absorption and bioavailability, making QASs promising candidates as active pharmaceutical ingredients (APIs) [6]. Nevertheless, despite numerous scientific reports describing QASs as effective bactericidal agents and topical drugs [7,8], their membrane permeability and pharmacokinetic profiles have not been sufficiently investigated.

Although most QASs are known to exhibit poor passive diffusion across biological membranes, some derivatives, such as the *N*-alkylisoquinolinium salts demonstrated unexpectedly high permeability, with sanguinarine reaching a permeability coefficient value of $4.2 \cdot 10^{-6}$ cm·s^{-1} [9]. This indicates that the passive transport of QASs is not always severely restricted, and that it is worth exploring compounds with physicochemical properties comparable to those of commercial drugs. Additionally, the conscious design of QASs and the use of naturally derived ions, such as B vitamins, namely nicotinamide (NA – known as precursor of NAD^+/$NADP^+$ coenzymes), nicotinic acid (NIC – popular cholesterol reducing drug) and *p*-aminobenzoic acid (PABA – recognized as precursor of ester-type local anesthetics, such as procaine and tetracaine), may enhance biocompatibility and safety, while leveraging the inherent biological relevance of these molecules. Noteworthy, PABA serves as a versatile scaffold in the design of various types of drugs and is also present in numerous pharmaceuticals with antimicrobial,

* Corresponding author at: Poznan University of Technology, Berdychowo 4, Poznan 61-131, Poland.
E-mail address: michal.niemczak@put.poznan.pl (M. Niemczak).
[1] orcid.org/0000-0002-4364-8267.

https://doi.org/10.1016/j.ejpb.2026.115100
Received 2 February 2026; Received in revised form 28 April 2026; Accepted 13 May 2026
Available online 17 May 2026

anticancer and anti-inflammatory properties [10]. NA and NIC play an important role in metabolism and exhibit anti-inflammatory effects [11,12].

A systematic evaluation of the effects of both alkyl chain length and counterion identity on pharmacokinetic properties is essential for rational drug design. Computational methods provide an efficient approach to this challenge, allowing rapid prediction of key pharmacokinetic parameters such as permeability coefficient (P_{app}) [13], intestinal absorption (IA) [14], fraction unbound (Fu) [15] and aqueous solubility at an early stage of drug development [16]. These predictions help identify promising candidates, allowing to eliminate unsuitable compounds before engaging in resource-intensive experimental studies. Complementing *in silico* screening, the Parallel Artificial Membrane Permeability Assay (PAMPA) offers a cost-effective, high-throughput experimental method to evaluate passive membrane permeability, enabling dynamic assessment of transport, avoiding, at this stage, *in vivo* or *ex vivo* studies [17,18]. The PAMPA method has proven to be a useful tool for assessing the permeability of hydrophobic compounds, demonstrating that for highly lipophilic molecules, a decrease in apparent permeability is observed due to the presence of the unstirred water layer (UWL) barrier and membrane retention [19]. Studies covering a wide range of compounds such as from peptides and agrochemicals, have confirmed that permeability in the PAMPA system decreases with increasing apparent lipophilicity, which is a consequence of the mentioned above phenomenon [20]. Furthermore, ion pairing of adefovir with ammonium salts, such as cetylpyridinium chloride (CPC) and cetrimide, has been shown to significantly increase its lipophilicity and permeability in the PAMPA system. The adefovir–CPC complex demonstrated a 2.5-fold greater permeability than adefovir alone, confirming the potential of this strategy to improve intestinal absorption of hydrophilic compounds [21]. Other QASs with a quinuclidine skeleton showed negligible permeability in the PAMPA assay despite the observed sorption on the membrane. However, these compounds did not have a typical amphiphilic structure – the long alkyl chain was attached to a carbon distant from the nitrogen atom – which resulted not only in their low permeability, but also in a different mechanism of bactericidal action compared to conventional QASs [22]. Although valuable, the available data are fragmentary and do not allow for a detailed explanation of the mechanism of penetration of QASs in the PAMPA system.

Interfacial behavior represents another critical factor influencing oral absorption. Surface activity, characterized by parameters such as surface tension (γ) and surface pressure (π), affects molecular interactions at lipid–water interfaces, which in turn can modulate membrane permeability [23]. Systematic investigation of these properties provides mechanistic insight into the relationship between molecular structure and absorption, offering predictive value for designing compounds with optimized bioavailability.

This study focuses on two series of QASs differing in counterions and alkyl chain lengths (**1**–**8**), alongside their nonionic counterparts (**[NA] [NIC]** and **[NA] [PABA]** lacking the alkyl chain), and the commercially used diclofenac sodium (DFC-Na). All chemical structures are depicted in Fig. 1. *In silico* pharmacokinetic predictions were followed by experimental evaluation of passive permeability using PAMPA at multiple time points (0.5, 1, 6 and 16 h). Finally, interfacial properties, including surface tension and surface pressure, were assessed to explore their correlation with permeability. By integrating computational and experimental approaches, this work aims to elucidate how alkyl chain length, counterion selection, and surface activity collectively influence the pharmacokinetic potential of vitamin B-based compounds, providing a framework for rational design of orally bioavailable and safe compounds.

2. Materials and methods

Materials: 1-Bromohexane, (99%), 1-bromooctane (99%), 1-bromodecane (98%), 1-bromododecane (97%), nicotinamide (98%), nicotinic

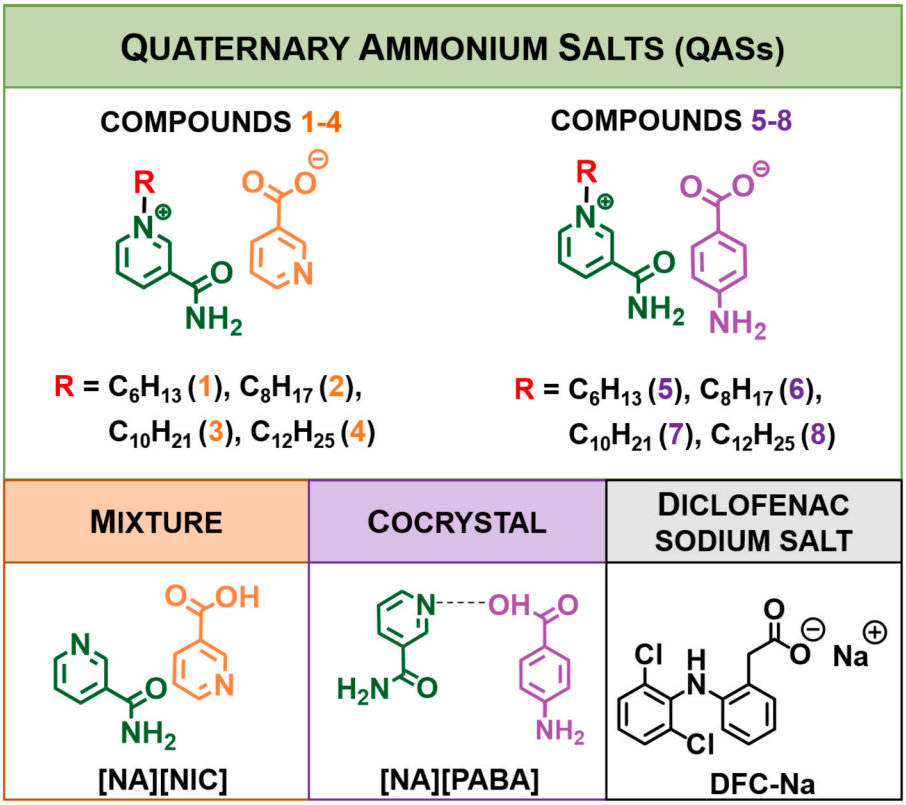

Fig. 1. Chemical structures of tested QASs (**1**–**8**), mixture of nicotinamide and nicotinic acid (**[NA] [NIC]**), nicotinamide and *p*-aminobenzoic acid cocrystal (**[NA] [PABA]**), and diclofenac sodium salt (**DFC-Na**).

acid (98%) and *p*-aminobenzoic acid (99%) were purchased from Sigma-Aldrich (Saint Louis, MO, USA). Methanol (99.8%), acetone (99%), *n*-propanol (99.5%), potassium hydroxide (99%) were obtained from Avantor (Gliwice, Poland) and used without further purification. *N*-hexylnicotinamide nicotinate (**1**), *N*-octylnicotinamide nicotinate (**2**), *N*-decylnicotinamide nicotinate (**3**), *N*-dodecylnicotinamide nicotinate (**4**), *N*-hexylnicotinamide *p*-aminobenzoate (**5**), *N*-octylnicotinamide *p*-aminobenzoate (**6**), *N*-decylnicotinamide *p*-aminobenzoate (**7**), *N*-dodecylnicotinamide *p*-aminobenzoate (**8**), mixture of nicotinamide and nicotinic acid **[NA] [NIC]**, nicotinamide and *p*-aminobenzoic acid cocrystal **[NA] [PABA]** were synthesized with high purity (HPLC – 98.5–99.7%, Table S1 in Supporting Information) according to the methodology presented in Supporting Information (page 2–3). The chemical structures of the tested compounds are shown in Fig. 1.

Diclofenac sodium (DFC-Na; 98.0%), soya lecithin (90.0%) and *n*-dodecane (99.0%) were purchased from Avantor (Gliwice, Poland) and used without further purification. Corning® Transwell® 12 well plates (0.4 μm pore size) with polycarbonate membrane were purchased from Merck (Darmstadt, Germany). Phosphate suffer saline (PBS) were purchased from Sigma-Aldrich (St. Louis, USA). Deionized water with a conductivity of < 0.1 μS cm^{-1}, from Hydrolab HLP Smart 1000 demineralizer (Straszyn, Poland) was used.

2.1. *In silico pharmacokinetics and toxicity prediction using Graph-Based Signatures (pkCSM)*

Pharmacokinetic and toxicity properties were predicted using pkCSM [24]. Predicted parameters included human intestinal absorption (IA), Caco-2 permeability and fraction unbound in plasma (Fu). All predictions were performed using the default settings of pkCSM. Aqueous solubility of the studied compounds was predicted using SwissADME [25]. Compounds' structures were converted into SMILES strings for analysis.

2.2. *Parallel artificial membrane permeability assay (PAMPA)*

The 12-well filter plate was used as the permeation donor and the 12-well receiver plate was used as the permeation acceptor. PBS buffer (pH 7.4) was used both as donor and acceptor medium throughout the study. A 2% (w/v) solution of lecithin in dodecane was prepared and carefully added (10 μL) into each well of the donor plate to form the hydrophobic filter material (0.40 μm) of the filter plate wells. Immediately after the application of the lipid layer, 0.7 mL of drug solution (1000 μg/mL in PBS) was added to each well of the donor plate. PBS (2.5 mL) was added to each well of the receptor plate. The drug-filled donor plate was then placed into the receptor plate, ensuring that the underside of the membrane was in direct contact with the buffer. The donor plate was coupled with the receptor plate, and the plate assembly was incubated at 37 °C without agitation for 0.5, 1, 6 and 16 h. The assembled plate was placed into a sealed container to minimize evaporation. After incubation, samples were withdrawn from acceptor wells. The drug concentration was determined by means of a VWR UV-6300PC spectrophotometer. Quantification was based on calibration curves prepared previously for each compound. Measurements were carried out at specific λ_{max} values: 262–264 nm for the nicotinate anion, 264–266 nm for the *p*-aminobenzoate anion, 262–263 nm for **[NA] [NIC]**, and 262–263 nm for **[NA] [PABA]**. Experiments were performed in triplicate. Mean values were used for data analysis. The permeability coefficients (P_{app}) were calculated using the following equations [26]:

$$P_{app} = -2.303 \times \frac{Vdn \times Vac}{Vdn + Vac} \times \frac{1}{S \times t} \times \log\left(1 - \frac{flux\%}{100}\right) \quad (1)$$

$$flux\% = \frac{ODac}{ODref} \times 100 \quad (2)$$

where:

Vdn – volume of the donor compartment (0.7 mL).
Vac – volume of the acceptor compartment (2.5 mL).
ODac – optical density of the solution of the acceptor compartment.
ODref – optical density of the reference solution
S – membrane area (1.13 cm^2).
t – incubation time (s).

2.3. *Surface tension (γ) and surface pressure (π)*

Surface tension (γ) was determined with the pendant drop method. The measurement device was a DSA 100 analyzer (Krüss, Germany, accuracy ± 0.01 $mN{\cdot}m^{-1}$) set at 25 °C (temperature controlled using a Fisherbrand FBH604 thermostatic bath – Fisher, with an accuracy of 0.1 °C). Analyzed compounds were dissolved in PBS to prepare solutions at an initial concentration of 1000 μg/mL. The principle of pendant drop method involves the formation of an axisymmetric drop at the tip of a syringe needle. A CCD camera records an image of the drop and the surface tension is calculated by analyzing the profile of the drop in accordance with the Laplace equation. The surface pressure (π) values were calculated according to Ollila *et al.* [27], using PBS as the reference medium following equation:

$$\pi = \gamma_0 - \gamma \quad (3)$$

where:

γ_0 – surface tension without surfactant.
γ – surface tension with surfactant.

3. Results and discussion

The combined *in silico*, PAMPA, and surface tension enabled a comprehensive examination of how alkyl chain length, counterion selection, and surface activity modulate the passive permeability of vitamin-B-derived ionic pairs. The investigated compounds comprised nicotinamide-derived QASs paired with either a nicotinate anion (**1**–**4**) or a *p*-aminobenzoate (PABA) (**5**–**8**). Within each series, the alkyl chain length was systematically varied, including hexyl (**1** and **5**), octyl (**2** and **6**), decyl (**3** and **7**), and dodecyl (**4** and **8**) derivatives. For comparative purposes, non-ionic reference systems, namely a mixture of nicotinamide and nicotinic acid (**[NA] [NIC]**), nicotinamide–PABA cocrystal (**[NA] [PABA]**), and the reference drug diclofenac sodium salt (DFC-Na), were also subjected to analyses. Notably, **[NA] [NIC]** and **[NA] [PABA]** were deliberately included to compare differences in membrane permeation between ionic and non-ionic systems. Together, the obtained results allowed to reveal clear structure–property relationships that rationalize the observed differences in transport and offer guidance for designing orally bioavailable amphiphilic active pharmaceutical ingredients.

3.1. *In silico pharmacokinetics and toxicity prediction using Graph-Based Signatures (pkCSM)*

In silico studies are playing an increasingly important role in the development of new drugs, allowing for preliminary assessment of their pharmacokinetic and toxicological properties without the need for costly and time-consuming *in vitro, in vivo or ex vivo* experiments. Parameters such as permeability through Caco-2 cells (P_{app}) and absorption in the human intestine (IA) make it possible to predict the oral bioavailability of compounds, which is crucial for pharmacological efficacy [28,29]. At the same time, the determination of the unbound fraction (Fu) provides information about its ability to interact with target sites [15,30]. Moreover, investigation of water solubility (WS) of orally administered drugs is crucial; poor solubility in gastrointestinal fluids often limits the dissolution, absorption and ultimately bioavailability of active ingredients [31]. Analysis of these parameters in

computer models allows to reveal the most promising candidates at an early stage of research, minimizing the risk of subsequent clinical failures. This approach enables more effective design of drugs with optimal pharmacokinetic properties and safety of use.

The results provided in Fig. 2 (as well as Fig. S1 and Table S2 in Supporting Information) show the computer calculation results of key pharmacokinetic parameters of selected QASs, providing insight into the potential of these compounds for oral drug administration. Permeability proved to be the most challenging parameter in assessing the potential of QASs as oral drugs. According to the data provided in Fig. 2A, QASs **3** and **4** exhibited high permeability coefficients (P_{app}), ca. $21 \cdot 10^{-6}$ cm·s^{-1}, showing significantly greater values compared to the reference compound – diclofenac sodium salt (DFC-Na, $P_{app} = 17 \cdot 10^{-6}$ cm·s^{-1}). This clearly indicates the high ability of some QASs to overcome biological barriers and potential superior bioavailability to commercially available ionic drugs. The length of the alkyl chain was found to be significantly important, particularly for QASs with chain lengths comprising at least 10 carbon atoms, which resulted in a pronounced increase in permeability for both studied anions. However, it should be emphasized that the intensity of the permeability increase strongly depends on the type of anion. In consequence, *p*-aminobenzoates with 10 and 12 carbon atoms in the alkyl moiety did not achieve as high P_{app} values (approx. $3 \cdot 10^{-6}$ cm·s^{-1}) as in the case of nicotinates. Notably, compounds with the shortest alkyl chains (**1** and **5**) exhibited significantly lower P_{app} values, ranging from 1.3 to $1.6 \cdot 10^{-6}$ cm·s^{-1}, which serves as the indicator of potentially limited permeability. Importantly, the P_{app} values for nonionic **[NA] [NIC]** and **[NA] [PABA]** were found to be the lowest (1.1 and $0.9 \cdot 10^{-6}$ cm·s^{-1}), emphasizing that the ionicity of the compound also determines *in silico* calculations regarding permeability.

As presented in Fig. 2B, the highest solubility in water was demonstrated by QAS **1**, reaching 141 mg·mL^{-1}. The lowest solubilities, however, were noted for **[NA] [NIC]** and **[NA] [PABA]** and, surprisingly, for DFC-Na, with values of 4.08, 2.39 and 0.00547 mg·mL^{-1}, respectively. Overall, the observed tendencies indicate that the alkyl chain elongation increases membrane permeability and decreases water solubility. Analysis of intestinal absorption (IA), which correlates drug bioavailability with its potential efficacy after oral administration, revealed moderate differences between the compounds studied (Fig. S1-A in Supporting Information). The highest values were observed for **3** and **4** (61.9 and 63.0%), which also had the highest membrane permeability (P_{app}), suggesting a synergistic effect of structural features that promote both permeability and absorption. Lower values were recorded for nonionic compounds: **[NA] [NIC]** and **[NA] [PABA]** (53.6%), while the reference drug DFC-Na had the highest absorption rate (77.0%), confirming its high pharmacokinetic efficacy. Overall, IA increased with increasing alkyl chain length. A reverse phenomenon was observed for the unbound fraction (Fu, Fig. S2-B), which exhibited a decreasing trend as the alkyl chain length increased. High Fu values are considered favorable, as it indicates that a significant proportion of the compound remains pharmacologically active, enabling effective distribution and target interaction while maintaining an acceptable pharmacokinetic profile. The highest Fu value was observed for QAS **1** (0.50), suggesting that almost half of the molecules remain in a free form, potentially pharmacologically available. Relatively high values were also achieved for **2** (0.42), **5** (0.41) and **[NA] [NIC]** (0.43), which may also promote a faster onset of action and higher distribution in tissues. In contrast, **3** and **4**, which had the highest permeability, showed significantly lower Fu values (0.34 and 0.25), suggesting stronger binding to plasma proteins. Interestingly, even lower values were recorded for DFC-Na (0.10), indicating a reduction in the free fraction and thus a potential impact on pharmacological availability, which can be concerning given its widespread use in modern pharmacology. The observed differences indicate that despite the high permeability of some compounds, their systemic efficacy may be modulated by the degree of protein binding.

Rezki *et al.* [32] investigated fluorinated pyridinium QASs with melting point below 100 °C, namely ionic liquids (ILs), functionalized with Schiff bases, including an assessment of their pharmacokinetic profile. Depending on their structural variations, gastrointestinal absorption was classified even as "High" (≥85%). Moreover, all compounds exhibited drug-like characteristics and favorable bioavailability profiles. The imidazolium ionic liquids with a benzothiazole amide function, on the other hand, showed excellent solubility in water. They were classified as soluble (33.3–100 mg·mL^{-1}) and moderately soluble (10–33.3 mg·mL^{-1}). One of the compounds in this group also showed good *in silico* absorption (81.75%) and high gastrointestinal absorption in accordance with ADME predictions [33]. Analyses of the permeability of gliclazide-based ILs revealed their effective permeability, with values ranging from $1.21 \cdot 10^{-6}$ to $1.53 \cdot 10^{-6}$ cm·s^{-1}, complying with the established requirements for orally administered drugs [13]. Together, these results indicate that appropriate structural modifications of QASs or ILs can enhance solubility, absorption, and overall bioavailability, confirming their potential as promising candidates for oral drug delivery. Nonetheless, our results demonstrate also that several key factors can be relatively easily adjusted by optimizing the alkyl chain length within the cation.

3.2. Parallel artificial membrane permeability assay (PAMPA)

Since its introduction in the late 1990s and widespread adoption in

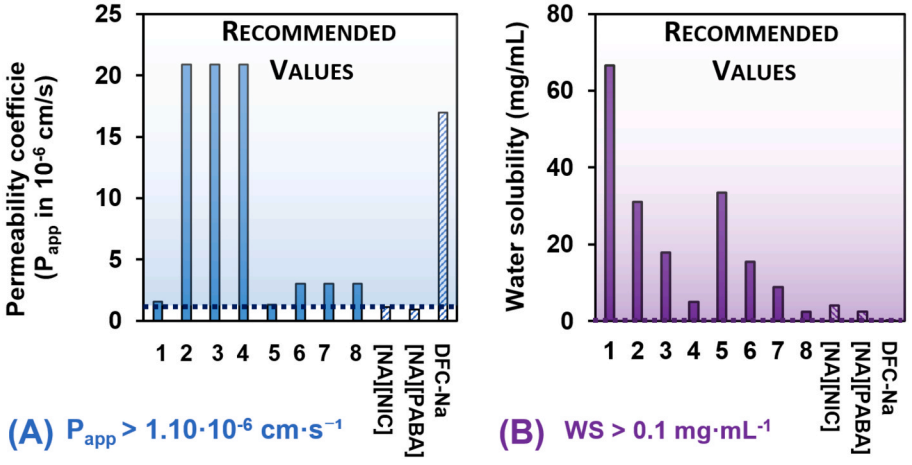

Fig. 2. Calculated values of permeability (A) and water solubility (B) for the studied compounds and DFC-Na. Colored zones indicate the minimum threshold for a candidate to be considered as a potentially effective drug [13,15,24,30,31].

the early 2000s, the PAMPA assay has become a widely used, rapid, and cost-effective method for evaluating passive diffusion across lipid membranes. Its simplicity, ease of standardization, and strong predictive value for passive membrane permeability make it an invaluable tool for early assessment of pharmacokinetic properties and potential oral bioavailability of new compounds [17]. It should be stressed that one of the critical methodological factors that can significantly affect the interpretation of permeability test results obtained using the PAMPA system is the presence of dimethyl sulfoxide (DMSO) in the test solutions [34–37]. Although DMSO is commonly used as a co-solvent facilitating the dissolution of compounds that are poorly soluble in water, its presence can significantly increase permeability through model membranes. This effect is mainly due to the specific properties of DMSO, which disrupt the lipid structure and alter its barrier properties. As a consequence, the use of DMSO may lead to an overestimation of the permeability coefficient (P_{app}), which in turn results in results that do not reflect actual physiological conditions. For this reason, it is essential to minimize its concentration or use alternative dissolution strategies (such as transformation of poorly soluble APIs into QASs or ILs) to maintain the reliability and comparability of data. Considering this effect, all compounds investigated in this study were analyzed without the addition of this (or any other) solvent, which enabled obtaining results more representative of the environment of the gastrointestinal tract.

The permeability coefficients determined via PAMPA assay after 6 h confirmed the high permeability potential of all analyzed compounds, as each of them met the required threshold of $P_{app} > 1.10 \cdot 10^{-6}$ cm·s^{-1} (Fig. 3 and Table S3 in Supporting Information).

In the case of the synthesized nicotinates (**1**–**4**), P_{app} values ranged from $4.7 \cdot 10^{-6}$ to $5.8 \cdot 10^{-6}$ cm·s^{-1}, with QAS **4** showing the highest permeability within this series. Although the overall permeability remained comparable to that of the reference drug DFC-Na ($P_{app} = 5.9 \cdot 10^{-6}$ cm·s^{-1}), a slight but clear dependence on alkyl chain length was evident. Interestingly, their nonionic analogue **[NA] [NIC]** showed permeability ($P_{app} = 5.8 \cdot 10^{-6}$ cm·s^{-1}) almost identical to DFC-Na, suggesting that in this case, the ionic nature did not significantly improve nor deteriorate transport across the model membrane.

On the other hand, obtained *p*-aminobenzoates (**5**–**8**) exhibited P_{app} values ranging from $4.2 \cdot 10^{-6}$ to $6.1 \cdot 10^{-6}$ cm·s^{-1}. Importantly, both **5** and its nonionic analogue **[NA] [PABA]** outperformed DFC-Na in permeability, achieving slightly higher P_{app} values, indicating favorable membrane transport behavior compared to this commercial drug. This enhanced diffusion most likely results from the optimal balance between polarity and lipophilicity provided by the PABA anion. Knowing that majority of QASs and ILs typically display very low permeability coefficients (P_{app} often far below $1 \cdot 10^{-6}$ cm·s^{-1}), the tested QASs exhibit exceptionally high permeability, far exceeding initial expectations. With P_{app} values more than 10–20 times higher than those of typical QASs, and comparable to or even exceeding that of diclofenac sodium, these molecules represent promising candidates for further *in vivo* studies in model organisms, such as rats or mice [9].

The assessment of penetration kinetics using the PAMPA system provides not only valuable information about a compound's ability to overcome biological barriers, but also allows to estimate and compare the rate of penetration of given substances over time. The data obtained represent an important link between physicochemical properties and pharmacokinetics, supporting the early selection of candidates with an appropriate bioavailability profile. The corresponding changes in permeability in time for the tested substances and DFC-Na, are presented in Fig. 4A and in Table S4 in Supporting Information. After 16 h, DFC-Na proved to be the most permeable drug, at 25.4%, with a steady increase within the analyzed range. Among nicotinic acid derivatives, **[NA] [NIC]** and QAS **4** showed the highest permeability values, 23.2% and 22.3%, respectively, which turned out to be comparable to those of the reference drug. On the other hand, the lowest permeability in the early phase was exhibited by **2**, particularly after 6 h. Nevertheless, its absorption gradually increased, aligning with other compounds after 16 h and reaching a maximum of 22.6%. Overall, permeability values showed a rapid increase during the first hour of incubation, and stabilization after 6 h, suggesting that a state of diffusion equilibrium had been reached. The differences between the early and late time points were statistically significant ($p < 0.05$, Table S5 in Supporting Information), while the lack of significance between periods of 6 and 16 h confirms a plateau.

On the other hand, for most *p*-aminobenzoic acid derivatives significant differences were observed between 6 and 16 h, indicating slower penetration kinetics and a delayed time of reaching a state of equilibrium (Fig. 4B and Table S6 in Supporting Information). This slower rate of permeation may be due to a lower lipophilicity that

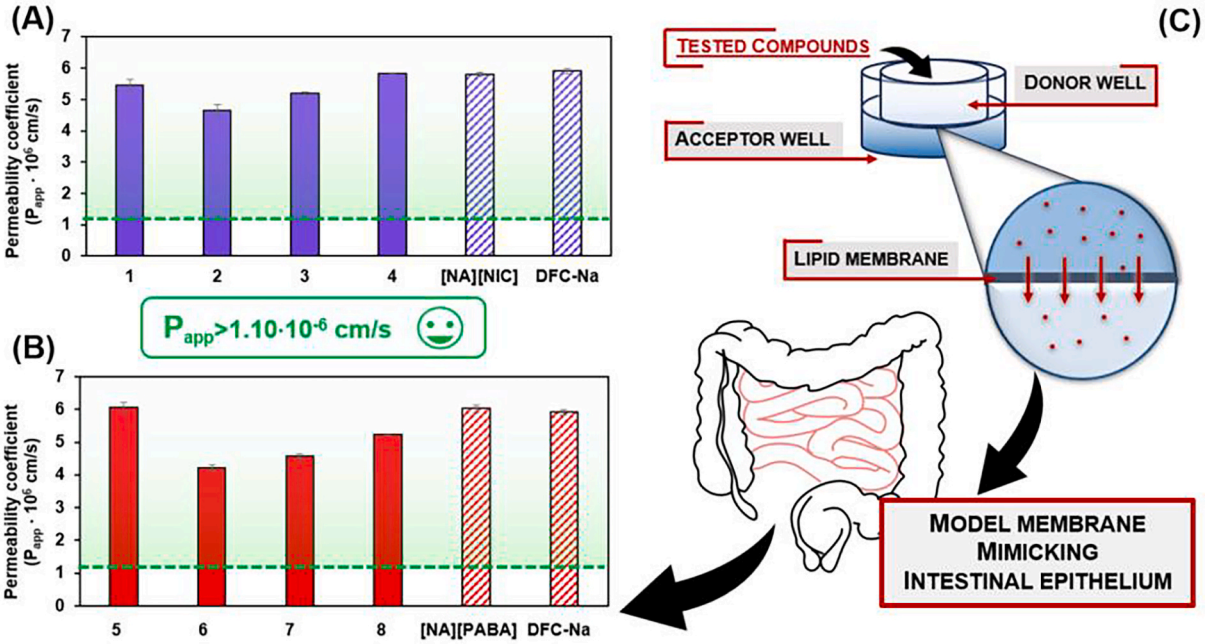

Fig. 3. Permeability coefficients of tested nicotinates (**A**) and *p*-aminobenzoates (**B**) determined after 6 h in comparison to DFC-Na; Scheme demonstrating principle and significance of the PAMPA assay (**C**).

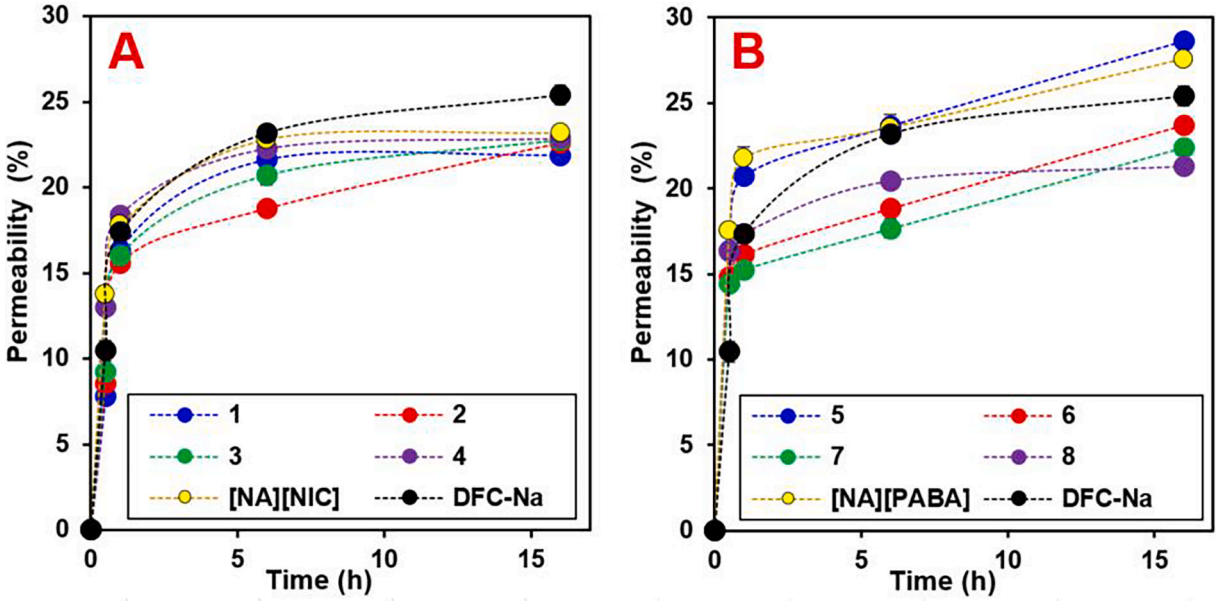

Fig. 4. Time-dependent permeability kinetics for tested nicotinates (**A**) and *p*-aminobenzoates (**B**) at a concentration of 1000 μg/mL in comparison to the reference compounds.

hinders interactions with the model membrane. **[NA] [PABA]** and the QAS with the shortest alkyl (**5**) showed the highest permeability values, after 16 h, reaching 27.6 and 28.6%, respectively. Remarkably, out of all ten molecules tested, only these two compounds surpassed the permeability of the reference drug DFC-Na. Interestingly, **5** showed better permeability compared to DFC-Na already at the earliest time point (0.5 h), maintaining this advantage throughout the permeation period. In contrast, the lowest initial permeability was observed for **7** and **8**, with values of 14.5 and 16.3%, accordingly, after 0.5 h. However, their permeability increased significantly over time, reaching 22.4 and 21.3% after 16 h. Overall, permeability values for all *p*-aminobenzoic acid derivatives increased gradually throughout the 16-hour incubation period, with statistically significant differences observed between early as well as later time points ($p < 0.05$, Table S7 in Supporting Information).

Performed kinetic analysis of the process revealed a complex and interesting relationship, according to which the permeation coefficient primarily reflects the initial rate of passive diffusion and is a kinetic parameter of transport across the membrane. The higher P_{app} values observed for nicotinate derivatives indicate faster permeation in the first hours of the experiment than their *p*-aminobenzoates counterparts. However, the permeation coefficient does not account for the thermodynamic aspect, namely the achievement of equilibrium between the donor and acceptor phases. Over longer incubation periods, *p*-aminobenzoates showed a systematic increase in permeation, while nicotinates quickly reached a plateau. This indicates that despite a faster initial diffusion, compounds containing PABA anion may ultimately achieve a higher overall permeation rate. Therefore, in the nicotinate series (Fig. 4A), all compounds, except **2,** reach equilibrium, whereas in the series *p*-aminobenzoates (Fig. 4B), a continuous, consistent increase in permeation is observed, with only DFC-Na and **8** reaching a plateau. Mechanistically, this can be explained by differences in alkyl chain length, steric factors and specific interaction between membrane and functional groups present in the selected anions. Compounds with longer alkyl chains exhibit faster initial diffusion, rapidly penetrate the lipid phase, and reach equilibrium, which favors a rapid plateau but limits overall permeability. In contrast, derivatives with shorter alkyl chains diffuse more slowly initially but maintain a steady increase in permeation over time, ultimately achieving a higher overall transport rate. This phenomenon likely results from lower steric hindrance and smaller molecular size, which facilitate continuous transport across the membrane after the more lipophilic analogs reach equilibrium.

Time-dependent penetration profiles were analyzed using various kinetic models to assess their suitability for describing the transdermal permeation of the selected QASs. Due to the absence of a distinct steady-state region and the rapid attainment of a plateau, classical diffusion-based linear fitting was not applicable to all compounds [38]. The data were therefore analyzed using both the Higuchi model and a saturable exponential (first-order kinetic) model, and the results are provided in Table S8 in the Supporting Information. For systems containing PABA (**5**–**8** and **[NA] [PABA]**), the Higuchi model provided a better fit ($R^2 = 0.88$–0.99), suggesting a diffusion-controlled permeation mechanism. In contrast, nicotinate-based compounds (**1**–**4** and **[NA] [NIC]**), as well as DFC-Na, were better described by the exponential model ($R^2 = 0.88$–0.98), indicating rapid initial permeation followed by early attainment of equilibrium. Furthermore, to enable quantitative comparison, the initial permeation rate (v_0) and permeation plateau (Q_p) were determined (Table S8 in the Supporting Information). Nicotinates (**1**–**4**) exhibited significantly higher initial permeation rates (10.8–17.1%·h^{-1}) compared to PABA (**5**–**8**) analogues (1.6–8.2%·h^{-1}), indicating faster membrane transport. Importantly, compounds **1** and **2** exhibited higher permeation rates than the reference DFC-Na (13.8%·h^{-1}), suggesting their potential for improved transdermal permeation. These findings demonstrate that the nature of the counterion in QASs strongly influences both the kinetics and mechanism of permeation.

Other analyses conducted in the PAMPA system concerning the permeability of the gliclazide-based IL showed its high effectiveness in penetrating biological membranes. The permeability coefficient values obtained ranged from $1.2 \cdot 10^{-6}$ to $1.5 \cdot 10^{-6}$ cm·s^{-1}, meeting the established criteria for substances intended for oral administration [13]. These results confirm the potential of gliclazide as an ionic compound with a favorable bioavailability profile, similar to the compounds investigated in this study. In contrast, studies of the permeability of oligosaccharides (agarobiose and agarohexose) in a human cell model showed lower P_{app} values, ranging from 0.2 to $0.4 \cdot 10^{-6}$ cm·s^{-1} [39]. Their limited ability to cross biological barriers again confirms the profound impact of molecular structure on transport processes and motivate to explore more deeply this type of fundamental mechanisms.

3.3. Surface tension

Undeniably, the investigation of the surface activity of aqueous solutions of amphiphilic compounds constitutes a crucial aspect to address their potential to penetrate the intestinal barrier. This originates from the fact that surface-active properties enable to modulate interactions between molecules and biological membranes [40]. Consequently, highly lipophilic substances demonstrating good surface activity properties can exhibit a higher affinity for the intestinal epithelium. This, in turn, contributes to enhance the drug solubility in intestinal fluids and promotes its permeability [41–43].

The surface activity of QASs **1**–**8** was evaluated by measuring the surface tension of their aqueous solutions at a concentration of 1000 μg/mL (1.0 g/L). Then, their surface properties were directly compared with the previously gathered permeability data, as shown in Fig. 5A and 5B, and in Table S4 and S6 in Supporting Information. The permeation percentage of nicotinate-based QASs ranged from 17.1% to 23.7% (Fig. 5A). The highest values were observed for QASs with the longest alkyl chain (**4** – 22.9%). Among the *p*-aminobenzoate series, the compound with the shortest alkyl chain (**5** – 23.7%, Fig. 5B) exhibited the higher permeability. Interestingly, a distinct decrease in permeability was observed in both groups for QASs with octyl chains (**2** and **6**), which exhibited the lowest values, accounting to 18.8% and 17.1%, respectively. This reduction was particularly pronounced within the *p*-aminobenzoate series, suggesting that increasing the molecular weight may limit diffusion by reducing molecular mobility across the lipid phase. In contrast, in the case of the nicotinate salts, this effect appears to be partially compensated by enhanced surface activity, which facilitates membrane interaction and promotes passive diffusion through the lipid layer – cf. Fig. 5C.

It should be noted that under the experimental conditions used in this study, the critical micellar concentration (CMC) of the tested surfactants was not reached. This conclusion is supported by additional surface tension measurements at concentrations up to 50% higher than those used in PAMPA permeability tests. For all compounds, no plateau in surface tension was observed, suggesting that the concentrations studied were insufficient for micelle formation. In consequence, interfacial saturation had not yet been reached even for compounds with a dodecyl alkyl chain, where surfactant molecules exist primarily as monomers and gradually adsorb to the interfacial interface. For this class of surfactants, the CMC value strongly depends on the alkyl chain length and amounts to approx. 54.6 g/L, 9.3 g/L, and 4.1 g/L for *N*-alkylnicotinamide bromides comprising octyl, decyl, dodecyl group, respectively [44]. Interestingly, literature reports on structurally similar long-chain pyridinium-based surfactants, viz. dodecyl-alkyl-3-methylpyridinium bromide, indicate a CMC of approximately 3.7 g/L. This value is comparable to that reported for alkylated nicotinamide derivatives of similar chain length, suggesting that the presence of an additional amide group has only a minor impact on this parameter [45].

As illustrated in Fig. 5A and 5B, surface tension values of QASs **1**–**8** ranged from 32.6 to 70.4 $mN{\cdot}m^{-1}$, with the highest values observed for **5** (70.4 $mN{\cdot}m^{-1}$) and **6** (67.2 $mN{\cdot}m^{-1}$), and the lowest for **4** (32.6 $mN{\cdot}m^{-1}$) and **8** (39.4 $mN{\cdot}m^{-1}$), accordingly. PBS, used as a reference solution, exhibited a surface tension as high as 71.60 $mN{\cdot}m^{-1}$. According to various reports, to promote increased permeability across biological membranes, a surfactant should exhibit a surface pressure (π) close to or higher than 25 $mN{\cdot}m^{-1}$ [23]. Surface pressure is defined as the difference between the surface tension of the pure solvent and that of the solvent with a monolayer of the substance. Accordingly, a low surface tension of a given solution correlates with a high surface pressure. Due to substantial differences in alkyl chain length, the calculated surface pressures of the tested QASs ranged notably from 1.2 to 39.0 $mN{\cdot}m^{-1}$ (Table S9 in Supporting Information). The collected data revealed that three QASs comprising 10 and 12 carbon atoms (**3**, **4** and **8**) meet this requirement. On the contrary, compounds comprising shorter alkyl moieties displayed surface pressure below this threshold (π = 1.2–13.8

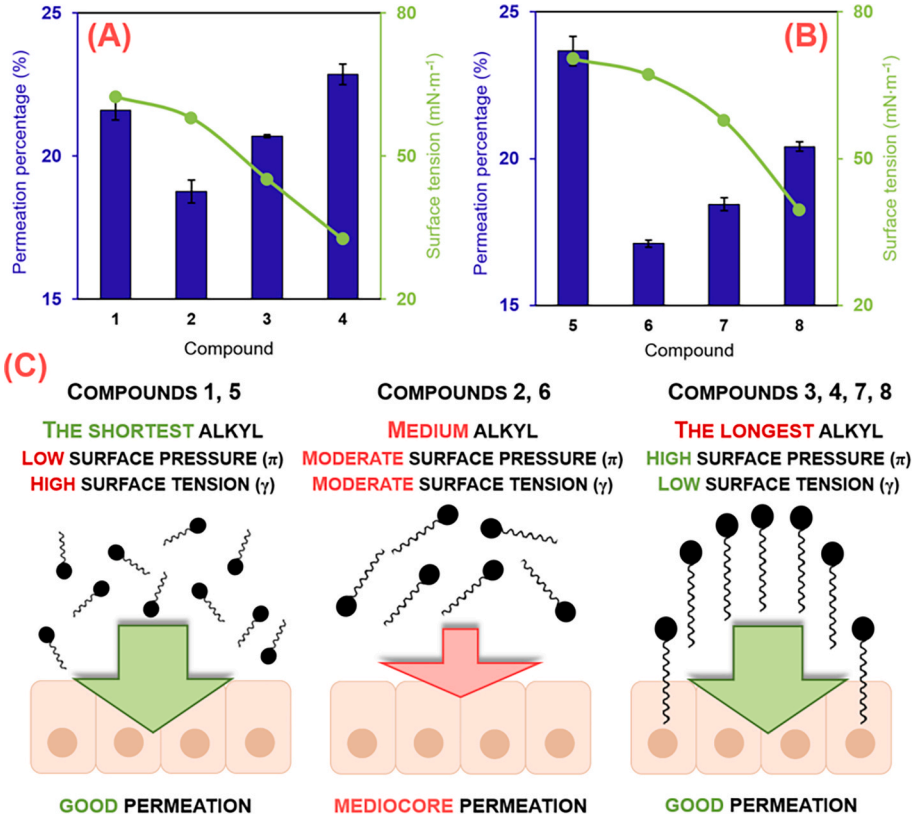

Fig. 5. Correlation between permeability coefficient (after 6 h) and surface tension for nicotinates (**A**) and *p*-aminobenzoates (**B**); proposed explanation of the effect of alkyl chain length on the permeability of QASs (**C**).

$mN \cdot m^{-1}$), indicating negligible or minimal impact on membrane permeability.

It should also be emphasized that an unforeseen correlation was discovered between molar mass and permeability among the studied QASs. In general, an increase in molar mass is associated with a decrease in permeability, which is consistent with the classical understanding that larger molecules diffuse more slowly through biological membranes. Studies of the intestinal permeability of agarose oligosaccharides conducted using Caco-2 cell models showed a time-dependent increase in plasma concentration, with an inverse correlation between plasma levels and molecular weight [39,46]. Similarly, studies of the effect of molecular weight on the oral absorption of water-soluble chitosan molecules, conducted in both human cells and rats, confirmed these observations, showing that an increase in molecular weight has a negative effect on oral absorption [47]. These findings emphasize that although molecular weight generally limits permeability, surface-active properties can modulate this relationship, leading to increased absorption under specific conditions. Nonetheless, analyzed QASs have shown that once surface activity is reached, permeability increases, regardless of the increasing molar mass. This phenomenon can be attributed to the ability of surface-active molecules to reduce interfacial tension, which facilitates transport through epithelial barriers. Intriguingly, in such cases, the effect of surface activity can counteract size-related diffusion limitations, leading to increased permeability.

Amphiphilic QASs gain the ability to lyse microbial cells; thus, longer alkyl chains could be also advantageous in the design of novel orally administered antibiotics with sufficient permeability thought the body. However, any potential human toxicity must be carefully balanced with the selection of alkyl chain length to maximize delivery of drug, while minimizing cytotoxicity. In this context, the tunable nature of QASs or ILs still opens versatile opportunities for optimizing bioavailability, membrane permeability and targeted pharmacological profiles, suggesting that they should not be overlooked and disregarded in future research on oral drug discovery.

4. Conclusions

This work focused on the evaluation of vitamin-B-based quaternary ammonium salts (QASs) and their nonionic counterparts for oral absorption, using *in silico* and experimental PAMPA assays. Computational predictions highlighted nicotinate derivatives as the most promising, with compounds **3** and **4** showing the highest apparent permeability ($21 \cdot 10^{-6}$ $cm \cdot s^{-1}$) and human intestinal absorption (61.9 and 63.0% respectively), while compounds **1** and **2** demonstrated the most favorable fraction unbound (0.50 and 0.42 accordingly) and water solubility (141.0 $mg \cdot mL^{-1}$ and 66.5 $mg \cdot mL^{-1}$). Experimental PAMPA results differed from *in silico* calculations particularly for nonionic moieties. In effect, performed studies confirmed high permeability of all compounds; within 6-hour period, their P_{app} values exceeded $1.10 \cdot 10^{-6}$ $cm \cdot s^{-1}$. Interestingly, the PAMPA results showed that QASs with the nicotinate anion exhibited permeability values comparable to diclofenac sodium salt (DFC-Na), whereas *p*-aminobenzoate derivatives, particularly compound **5** and its nonionic analogue **[NA] [PABA]**, slightly outperformed the reference drug. These findings suggest that ionic interactions do not necessarily enhance permeability, and that molecular structure and anion specificity play a decisive role in regulating passive diffusion across the membrane. Moreover, time-resolved studies of PAMPA showed that nicotinate derivatives (except **2**) and DFC-Na reached a permeability plateau after 6 h, whereas PABA derivatives showed a continuous increase after that period of time. This trend reflects chain-length-dependent diffusion dynamics, where longer alkyl chains promote faster equilibrium, while shorter ones sustain a slower but overall more efficient permeation process. Surface tension studies revealed that once surface activity is reached, permeability increases regardless of the molar mass, as surface-active molecules reduce interfacial tension and facilitate transport. Overall, alkyl chain length, counterion selection, and surface activity synergistically govern the passive permeability of the studied QASs, making them particularly promising candidates for oral drug development.

CRediT authorship contribution statement

Adriana Olejniczak: Writing – original draft, Visualization, Methodology, Investigation, Funding acquisition, Formal analysis, Data curation, Conceptualization. **Mara G. Freire:** Writing – review & editing, Funding acquisition. **Michał Niemczak:** Writing – review & editing, Supervision, Resources, Methodology, Funding acquisition, Conceptualization.

Declaration of competing interest

The authors declare that they have no known competing financial interests or personal relationships that could have appeared to influence the work reported in this paper.

Acknowledgment

This research was funded by the Ministry of Science and Higher Education as a subsidy to Poznan University of Technology in Poland (0912/SBAD/2504) and by the 'PhDBoost' Program for doctoral students of the Doctoral School of Poznan University of Technology (in 2024) from the University's subsidy financed from the funds of Ministry of Science and Higher Education (0912/SPHD/2521). This work was developed within the scope of the project CICECO Aveiro Institute of Materials, UID/50011/2025 (DOI 10.54499/UID/50011/2025) & LA/P/0006/2020 (DOI 10.54499/LA/P/0006/2020), financed by national funds through the FCT/MCTES (PIDDAC).

Appendix A. Supplementary data

Supplementary data to this article can be found online at https://doi.org/10.1016/j.ejpb.2026.115100.

Data availability

Data will be made available on request.

References

[1] J. Lou, H. Duan, Q. Qin, Z. Teng, F. Gan, X. Zhou, X. Zhou, Advances in Oral Drug delivery Systems: challenges and Opportunities, Pharmaceutics 15 (2023) 484, https://doi.org/10.3390/pharmaceutics15020484.
[2] M. Niemczak, D.K. Kaczmarek, T. Klejdysz, D. Gwiazdowska, K. Marchwińska, J. Pernak, Ionic Liquids Derived from Vitamin C as Multifunctional active Ingredients for Sustainable Stored-Product Management, ACS Sustain. Chem. Eng. 7 (2019) 1072–1084, https://doi.org/10.1021/acssuschemeng.8b04696.
[3] D. Pęziak-Kowalska, F. Fourcade, M. Niemczak, A. Amrane, Ł. Chrzanowski, G. Lota, Removal of herbicidal ionic liquids by electrochemical advanced oxidation processes combined with biological treatment, Environ. Technol. 38 (2017) 1093–1099, https://doi.org/10.1080/09593330.2016.1217941.
[4] A. Brzęczek-Szafran, P. Więcek, M. Guzik, A. Chrobok, Combining amino acids and carbohydrates into readily biodegradable, task specific ionic liquids, RSC Adv. 10 (2020) 18355–18359, https://doi.org/10.1039/D0RA03664A.
[5] A. Olejniczak, W. Stachowiak, T. Rzemieniecki, M. Niemczak, Adjustment of the Structure of the Simplest Amino Acid present in Nature—Glycine, toward more Environmentally Friendly Ionic Forms of Phenoxypropionate-based Herbicides, Int. J. Mol. Sci. 24 (2023), https://doi.org/10.3390/ijms24021360.
[6] A. Olejniczak, W. Stachowiak, D. Ziental, J. Długaszewska, T. Rzemieniecki, M. Wysokowski, T. Jesionowski, M. Niemczak, Unraveling the potential of Vitamin B3-Derived Salts with a Salicylate Anion as Dermal active Agents for Acne Treatment, Mol. Pharm. 21 (2024) 4634–4647, https://doi.org/10.1021/acs.molpharmaceut.4c00543.
[7] A.Q. Pedro, L.S. Castro, J.A.P. Coutinho, M.G. Freire, Ionogels as advanced materials for overcoming challenges in wound healing and drug delivery, Nano Mater. Sci. 7 (2025) 599–626, https://doi.org/10.1016/j.nanoms.2024.06.010.
[8] W.A. Arnold, A. Blum, J. Branyan, T.A. Bruton, C.C. Carignan, G. Cortopassi, S. Datta, J. DeWitt, A.C. Doherty, R.U. Halden, H. Harari, Quaternary ammonium compounds: a chemical class of emerging concern, Environ. Sci. Technol. 57 (20) (2023) 7645–7665, https://doi.org/10.1021/acs.est.2c08244.

[9] H. Fischer, M. Kansy, A. Avdeef, F. Senner, Permeation of permanently positive charged molecules through artificial membranes—Influence of physico-chemical properties, Eur. J. Pharm. Sci. 31 (2007) 32–42, https://doi.org/10.1016/j.ejps.2007.02.001.
[10] F. Haroon, U. Farwa, M. Arif, M.A. Raza, Z.A. Sandhu, M. El Oirdi, M. Farhan, M. A. Alhasawi, Novel Para-Aminobenzoic Acid Analogs and their potential Therapeutic applications, Biomedicines 11 (2023) 2686, https://doi.org/10.3390/biomedicines11102686.
[11] A.M. Godin, W.C. Ferreira, L.T.S. Rocha, R.G. Ferreira, A.L.L. Paiva, L.A. Merlo, E. B. Nascimento, L.F.S. Bastos, M.M. Coelho, Nicotinic acid induces antinociceptive and anti-inflammatory effects in different experimental models, Pharmacol. Biochem. Behav 101 (2012) 493–498, https://doi.org/10.1016/j.pbb.2012.02.012.
[12] L. Camillo, E. Zavattaro, P. Savoia, Nicotinamide: A multifaceted molecule in skin health and beyond, Medicina 61 (2) (2025) 254, https://doi.org/10.3390/medicina61020254.
[13] B. Zhou, D. Teng, J. Li, Y. Zhang, M. Qi, M. Hong, G.-B. Ren, Development of a gliclazide ionic liquid and its mesoporous silica particles: an effective formulation strategy to improve oral absorption properties, RSC Adv. 12 (2022) 1062–1076, https://doi.org/10.1039/D1RA07499G.
[14] M.A.C. Pérez, M.B. Sanz, L.R. Torres, R.G. Ávalos, M.P. González, H.G. Díaz, A topological sub-structural approach for predicting human intestinal absorption of drugs, Eur. J. Med. Chem. 39 (2004) 905–916, https://doi.org/10.1016/j.ejmech.2004.06.012.
[15] L. Di, An update on the importance of plasma protein binding in drug discovery and development, Expert Opin. Drug Discov. 16 (2021) 1453–1465, https://doi.org/10.1080/17460441.2021.1961741.
[16] S.Q. Pantaleão, P.O. Fernandes, J.E. Gonçalves, V.G. Maltarollo, K.M. Honorio, Recent advances in the Prediction of Pharmacokinetics Properties in Drug Design Studies: a Review, ChemMedChem 17 (2022) e202100542, https://doi.org/10.1002/cmdc.202100542.
[17] H. Li, H. Zeng, D. He, M. Wang, L. Liu, W. Liang, Y. Shu, S. Zhao, G. Sun, C. Lv, C. Xiao, Y. Liu, A new approach to examining the extraction process of Zhishi and Zhiqiao considering the synergistic effect of complex mixtures by PAMPA, J. Chromatogr. B 1099 (2018) 10–17, https://doi.org/10.1016/j.jchromb.2018.09.017.
[18] B. Sinkó, T.M. Garrigues, G.T. Balogh, Z.K. Nagy, O. Tsinman, A. Avdeef, K. Takács-Novák, Skin–PAMPA: a new method for fast prediction of skin penetration, Eur. J. Pharm. Sci. 45 (2012) 698–707, https://doi.org/10.1016/j.ejps.2012.01.011.
[19] M. Fujikawa, K. Nakao, R. Shimizu, M. Akamatsu, QSAR study on permeability of hydrophobic compounds with artificial membranes, Bioorg. Med. Chem. 15 (2007) 3756–3767, https://doi.org/10.1016/j.bmc.2007.03.040.
[20] M. Akamatsu, M. Fujikawa, K. Nakao, R. Shimizu, In silico Prediction of Human Oral Absorption based on QSAR analyses of PAMPA Permeability, Chem. Biodivers. 6 (2009) 1845–1866, https://doi.org/10.1002/cbdv.200900112.
[21] B. Darsazan, A. Shafaati, A. Zarghi, S.A. Mortazavi, Evaluation of Ion-pair Formation of Adefovir to Improve Permeation across Artificial and Biological Membranes., J. Pharm. Pharm. Sci. a Publ. can. Soc. Pharm. Sci. Soc. can. Des, Sci. Pharm. 21 (2018) 160–170, https://doi.org/10.18433/jpps29394.
[22] D. Crnčević, L. Krce, Z. Brkljača, M. Cvitković, S. Babić Brčić, R. Čož-Rakovac, R. Odžak, M. Šprung, A dual antibacterial action of soft quaternary ammonium compounds: bacteriostatic effects, membrane integrity, and reduced in vitro and in vivo toxicity, RSC Adv. 15 (2025) 1490–1506, https://doi.org/10.1039/D4RA07975B.
[23] W.J. Xia, H. Onyuksel, Mechanistic Studies on Surfactant-Induced Membrane Permeability Enhancement, Pharm. Res. 17 (2000) 612–618, https://doi.org/10.1023/A:1007581202873.
[24] D.E.V. Pires, T.L. Blundell, D.B. Ascher, pkCSM: predicting Small-Molecule Pharmacokinetic and Toxicity Properties using Graph-based Signatures, J. Med. Chem. 58 (2015) 4066–4072, https://doi.org/10.1021/acs.jmedchem.5b00104.
[25] A. Daina, O. Michielin, V. Zoete, SwissADME: a free web tool to evaluate pharmacokinetics, drug-likeness and medicinal chemistry friendliness of small molecules, Sci. Rep. 7 (2017) 42717, https://doi.org/10.1038/srep42717.
[26] K. Sugano, H. Hamada, M. Machida, H. Ushio, High Throughput Prediction of Oral Absorption: Improvement of the Composition of the Lipid solution used in Parallel Artificial Membrane Permeation Assay, SLAS Discov. 6 (2001) 189–196, https://doi.org/10.1177/108705710100600309.
[27] O.H.S. Ollila, A. Lamberg, M. Lehtivaara, A. Koivuniemi, I. Vattulainen, Interfacial Tension and Surface pressure of High Density Lipoprotein, Low Density Lipoprotein, and Related Lipid Droplets, Biophys. J. 103 (2012) 1236–1244, https://doi.org/10.1016/j.bpj.2012.08.023.
[28] T. Hou, J. Wang, W. Zhang, X. Xu, ADME Evaluation in Drug Discovery. 7. Prediction of Oral Absorption by Correlation and Classification, J. Chem. Inf. Model. 47 (2007) 208–218, https://doi.org/10.1021/ci600343x.
[29] Y. Kamiya, H. Takaku, R. Yamada, C. Akase, Y. Abe, Y. Sekiguchi, N. Murayama, M. Shimizu, M. Kitajima, F. Shono, K. Funatsu, H. Yamazaki, Determination and prediction of permeability across intestinal epithelial cell monolayer of a diverse range of industrial chemicals/drugs for estimation of oral absorption as a putative marker of hepatotoxicity, Toxicol. Reports 7 (2020) 149–154, https://doi.org/10.1016/j.toxrep.2020.01.004.
[30] A. Treyer, S. Walday, H. Boriss, P. Matsson, P. Artursson, A Cell-Free Approach based on Phospholipid Characterization for Determination of the Cell specific Unbound Drug Fraction (fu,cell), Pharm. Res. 36 (2019) 178, https://doi.org/10.1007/s11095-019-2717-1.
[31] J. van der Merwe, J. Steenekamp, D. Steyn, J. Hamman, The Role of Functional Excipients in Solid Oral Dosage Forms to Overcome Poor Drug Dissolution and Bioavailability, Pharmaceutics 12 (2020) 393, https://doi.org/10.3390/pharmaceutics12050393.
[32] N. Rezki, S.A. Al-Sodies, M. Messali, S.K. Bardaweel, P.K. Sahu, F.F. Al-blewi, P. K. Sahu, M.R. Aouad, Identification of new pyridinium ionic liquids tagged with Schiff bases: Design, synthesis, in silico ADMET predictions and biological evaluations, J. Mol. Liq. 264 (2018) 367–374, https://doi.org/10.1016/j.molliq.2018.05.071.
[33] F. Al-blewi, N. Rezki, A. Naqvi, H. Qutb Uddin, S. Al-Sodies, M. Messali, M. R. Aouad, S. Bardaweel, A Profile of the In Vitro Anti-Tumor activity and In Silico ADME predictions of Novel Benzothiazole Amide-Functionalized Imidazolium Ionic Liquids, Int. J. Mol. Sci. 20 (2019) 2865, https://doi.org/10.3390/ijms20122865.
[34] M. Di Stefano, S. Masoni, G. Bononi, G. Poli, S. Galati, F. Gado, S. Manzi, C. Vagaggini, A. Brai, I. Caligiuri, K. Asif, F. Rizzolio, M. Macchia, A. Chicca, A. Sodi, V. Di Bussolo, F. Minutolo, P. Meier, J. Gertsch, C. Granchi, E. Dreassi, T. Tuccinardi, Design, synthesis, ADME and biological evaluation of benzylpiperidine and benzylpiperazine derivatives as novel reversible monoacylglycerol lipase (MAGL) inhibitors, Eur. J. Med. Chem. 263 (2024) 115916, https://doi.org/10.1016/j.ejmech.2023.115916.
[35] A. Gitlin-Domagalska, A. Olejnik, J. Ruczyński, D. Starego, N. Ptaszyńska, A. Łęgowska, D. Dębowski, C. Gilon, K. Rolka, Application of Lipophilic Prodrug Charge Masking Strategy to Obtain Novel, potential Oxytocin Prodrugs, Int. J. Mol. Sci. 26 (2025) 4772, https://doi.org/10.3390/ijms26104772.
[36] J. Bošković, V. Dobričić, J. Savić, J. Rupar, M. Aleksić, B. Marković, O. Čudina, In Vitro Evaluation of Pharmacokinetic Properties of selected dual COX-2 and 5-LOX Inhibitors, Pharmaceuticals 17 (2024) 1329, https://doi.org/10.3390/ph17101329.
[37] D. Bai, Z. Schelz, D. Erdős, A.K. Kis, V. Nagy, I. Zupkó, G.T. Balogh, Z. Szakonyi, Stereoselective Synthesis and Antiproliferative Activities of Tetrafunctional Diterpene Steviol Derivatives, Int. J. Mol. Sci. 24 (2023) 1121, https://doi.org/10.3390/ijms24021121.
[38] M. Askarizadeh, N. Esfandiari, B.B. Honarvar, S.A. Sajadian, A. Azdarpour, Kinetic Modeling to Explain the Release of Medicine from Drug delivery Systems, ChemBioEng Rev. 10 (2023) 1006–1049, https://doi.org/10.1002/cben.202300027.
[39] I. Shirai, K. Karasawa, Y. Kodaira, Y. Iwasaki, Y. Shigemura, H. Makabe, S. Katayama, Intestinal permeability of agaro-oligosaccharides: Transport across Caco-2 cell monolayers and pharmacokinetics in rats, Front. Nutr. 9 (2022) 996607. https://www.frontiersin.org/journals/nutrition/articles/10.3389/fnut.2022.996607.
[40] S. Schreier, S.V.P. Malheiros, E. de Paula, Surface active drugs: self-association and interaction with membranes and surfactants. Physicochemical and biological aspects, Biochim. Biophys. Acta - Biomembr. (1508 (2000)) 210–234, https://doi.org/10.1016/S0304-4157(00)00012-5.
[41] R.N. Waterhouse, Determination of lipophilicity and its use as a predictor of blood–brain barrier penetration of molecular imaging agents, Mol. Imaging Biol. 5 (2003) 376–389, https://doi.org/10.1016/j.mibio.2003.09.014.
[42] J.H. Fagerberg, P. Zarmpi, H. Jabbar, N. Fotaki, Affinity of Lipophilic Drugs to mixed Lipid Aggregates in simulated Gastrointestinal Fluids, J. Pharm. Sci. 110 (2021) 186–197, https://doi.org/10.1016/j.xphs.2020.09.053.
[43] A. Lindahl, B. Persson, A.-L. Ungell, H. Lennernäs, Surface activity and Concentration Dependent Intestinal Permeability in the Rat, Pharm. Res. 16 (1999) 97–102, https://doi.org/10.1023/A:1018879014281.
[44] K. Kalyanasundaram, T. Colassis, R. Humphry-Baker, P. Savarino, E. Barni, E. Pelizzetti, M. Grätzel, Micellar properties of nicotinamide-based surfactants, J. Colloid Interface Sci. 132 (1989) 469–474, https://doi.org/10.1016/0021-9797(89)90261-0.
[45] D. Fu, X. Gao, B. Huang, J. Wang, Y. Sun, W. Zhang, K. Kan, X. Zhang, Y. Xie, X. Sui, Micellization, surface activities and thermodynamics study of pyridinium-based ionic liquid surfactants in aqueous solution, RSC Adv. 9 (2019) 28799–28807, https://doi.org/10.1039/C9RA04226A.
[46] C.R. Pye, W.M. Hewitt, J. Schwochert, T.D. Haddad, C.E. Townsend, L. Etienne, Y. Lao, C. Limberakis, A. Furukawa, A.M. Mathiowetz, D.A. Price, S. Liras, R. S. Lokey, Nonclassical size Dependence of Permeation Defines Bounds for Passive Adsorption of Large Drug Molecules, J. Med. Chem. 60 (2017) 1665–1672, https://doi.org/10.1021/acs.jmedchem.6b01483.
[47] S.Y. Chae, M.-K. Jang, J.-W. Nah, Influence of molecular weight on oral absorption of water soluble chitosans, J. Control. Release 102 (2005) 383–394, https://doi.org/10.1016/j.jconrel.2004.10.012.